

1 **Age-related differences in electrophysiological** 2 **correlates of visuospatial reorientation**

3 Clément Naveilhan¹, Alexandre Delaux², Marion Durteste², Jerome Lebrun³,
4 Raphaël Zory^{1,4}, Angelo Arleo², Stephen Ramanoël^{1,2,*}

5 ¹ Université Côte d'Azur, LAMHES, Nice, France

6 ² Sorbonne Université, INSERM, CNRS, Institut de la Vision, 17 rue Moreau, F-75012 Paris,
7 France

8 ³ Université Côte d'Azur, Laboratoire I3S, CNRS, Nice, France

9 ⁴ Institut Universitaire de France (IUF), Paris, France

10 *CA, Corresponding Author: Dr. Stephen Ramanoël

11 Mail: stephen.ramanoel@univ-cotedazur.fr

12 Number of figures: 5

13 Abstract

14 Spatial navigation abilities decline with age. Recent studies revealed a specific impairment in landmark-
15 based reorientation, linked to changes in scene-selective brain regions activity. While fMRI studies
16 suggest that these cortical modulations might be compensatory, a more precise investigation of the brain
17 dynamics associated with visuospatial processing is warranted. We analyzed Event-Related Potentials
18 and Event-Related Spectral Perturbations recorded from electrodes over scene-selective regions. 28
19 young adults and 28 older adults completed a desktop-based reorientation task using landmarks. Our
20 findings show poorer reorientation performance among older adults. Signatures of age-related
21 modulation of EEG activity imputable to scene-selective regions were predominantly observed within
22 the right hemisphere. EEG analysis disclosed a tripartite worsening of scene processing accounting for
23 older adults' difficulties. Firstly, a delayed and reduced P1 component likely reflects a slower and less
24 efficient stimulus discrimination. Secondly, an increased N1 amplitude and theta-band activity suggest
25 a higher demand on cognitive resources associated with more effortful processing of visuospatial
26 information. Thirdly, a decreased P2 amplitude may imply deficient attentional mechanisms to select
27 task-relevant stimuli.

28 Keywords:

29 Aging; ERP; ERSP; Spatial navigation; Visuospatial task; Landmarks

30 1. Introduction

31 Spatial navigation encompasses a complex set of behaviors that allow us to find our way and move in
32 our environment. Although we are able to perform it effortlessly on a daily basis, successful navigation
33 requires intricate cognitive processes such as sensory cue integration, working memory, or path
34 integration (Wolbers & Hegarty, 2010), which are supported by a large and highly interconnected
35 cerebral network (Ekstrom et al., 2017; Julian et al., 2018). Healthy aging is causally involved in the
36 decline of spatial navigation abilities (Lester et al., 2017), with older adults experiencing difficulty in
37 navigating both familiar and unfamiliar environments (Barrash, 1994). These impairments reduce the
38 autonomy and mobility of older adults (Burns, 1999) resulting in an increased risk of progression of
39 age-related disorders such as Alzheimer's disease (Coughlan et al., 2018). Given the general aging of
40 the population, it is essential to gain a better understanding of the factors contributing to these age-
41 related navigational deficits and their neural correlates.

42 Among all the information required for spatial navigation, the ability to perceive and integrate
43 visuospatial information plays a crucial role for humans who depend predominantly on their visual
44 system to interact with their surroundings (Ekstrom, 2015; Foo et al., 2005). Vision allows humans to
45 recognize the environmental context in which they are navigating and to rapidly encode the navigability
46 of a visual scene presented (Greene & Oliva, 2009). The extraction of visual landmarks that provide
47 information-rich cues for their orientation is also sustained by this sensory modality, allowing an
48 efficient human spatial navigation (Fischer et al., 2020). Authors have observed that greater visual
49 attention is indeed devoted to these landmarks, which subsequently serve as crucial reference points for
50 successful navigational behavior (de Condappa & Wiener, 2014; Hamid et al., 2010; Wenzel et al.,
51 2017). However, the ability to use landmark information for navigation declines with age, as evidenced
52 by several studies (Harris & Wolbers, 2012; Hartmeyer et al., 2017; Wiener et al., 2012). More recently,
53 Bécu et al. (2023) extended these findings by unveiling a specific decline in landmark-based navigation
54 (*i.e.*, encoding objects) but a preserved performance during geometry-based navigation (*i.e.*, encoding
55 spatial layouts). These two navigation modalities exhibit specific neural signatures in young adults
56 (Ramanoël et al., 2022) highlighting the importance of considering their neural correlates to gain insight
57 into the specific deficits of older adults in landmark navigation.

58 The integration of spatial visual cues is mediated by a network of high-level visual brain regions. This
59 network comprises three scene-selective regions: the Parahippocampal Place Area (PPA) (Epstein &
60 Kanwisher, 1998), the Retrosplenial Complex (RSC, also referred as Medial Place Area, MPA)
61 (Maguire, 2001; Silson et al., 2016), and the Occipital Place Area (OPA) (Dilks et al., 2013). The PPA,
62 located in the parahippocampal cortex, is thought to be involved in the representation of the spatial
63 layout (Kravitz et al., 2011) and in landmark recognition (Janzen & van Turennout, 2004; Sun et al.,
64 2021), thus contributing to scene categorization (Persichetti & Dilks, 2018). The RSC, a region of the
65 posterior cingulate cortex, is involved in the computation of heading directions (Gramann et al., 2021;

66 Marchette et al., 2014), the translation of information between egocentric and allocentric spatial
67 reference frames (Vann et al., 2009; Zhang et al., 2012), and it may also combine visual and motor
68 inputs for landmark encoding (Fischer et al., 2020). Finally, the OPA, which is located near the
69 transverse occipital sulcus, supports first-person vision-guided navigation through its role in encoding
70 environmental boundaries, local elements, and potential paths in a scene, which are also called
71 navigational affordances (Bonner & Epstein, 2017; Epstein et al., 2017; Julian et al., 2018).

72 In the context of aging, several functional magnetic resonance imaging (fMRI) studies have highlighted
73 age-related modifications in scene-selective regions during visual and spatial processing. Notably,
74 reduced activity in the PPA has been observed to underpin age-related differences in the categorization
75 of the fine-grained content of visual scenes (Ramanoël et al., 2015). Furthermore, the neural specificity
76 and distinctiveness of the PPA and RSC have been shown to decline with age and to predict individual
77 source and spatial memory abilities (Koch et al., 2020; Srokova et al., 2020). Regarding the OPA, fMRI
78 acquisitions during a Y-maze reorientation task using objects as landmarks showed an increased activity
79 of this region in older adults (Ramanoël et al., 2020). Critically, this age-related increase in parietal
80 activity was only reported during the reorientation phase of the task involving landmark processing but
81 not during free navigation (not involving reorientation). This finding was complemented by another
82 brain connectivity study reporting a preserved structural connectivity around the OPA region and an
83 increased functional connectivity between the OPA and PPA in older adults (Ramanoël et al., 2019).

84 Despite these results, how the temporal dynamics of scene-selective regions could contribute to the age-
85 related navigational decline remains poorly characterized, mainly due to the limitations of fMRI in
86 capturing brain processes at the millisecond timescale (Glover, 2011). With its high temporal resolution,
87 Event-Related Potential (ERP) analysis represents a valuable neuroimaging approach for investigating
88 early perceptual processes with electroencephalography (EEG). Notably, one ERP component, the
89 occipito-parietal P2, has been proposed to be a marker of scene processing (Harel et al., 2016) and to
90 reflect the activity of scene-selective regions (Kaiser et al., 2020). These results were complemented
91 with intracranial EEG recordings suggesting that the activity of the OPA occurs in the time period of
92 the P2 component (Vlcek et al., 2020). Recently, the amplitude of the P2 component was reported to
93 scale linearly with the number of navigational affordances (Harel et al., 2022) reinforcing the P2 as a
94 marker of scene-selective activity and more specifically of the OPA. Based on recordings from these
95 occipito-parietal electrodes, Lithfous et al. (2014) reported an age-related increase of the P2 component
96 amplitude and delayed P2 latency associated with an impaired performance on a spatial localization
97 task. They suggested that changes of the parietal P2 component may reflect the mechanisms underlying
98 the age-related decline in spatial processing and they emphasized the need for further studies to
99 investigate P2 in relation to spatial memory or spatial visual cue processing. In a subsequent study using
100 an EEG time-frequency analysis, Lithfous et al. (2018) found an increase in parahippocampal *theta*
101 activity in high-performing older adults compared to young adults during a spatial navigation task. They

102 also found a decreased *theta* power in the group of low-performing older adult (*i.e.*, the group with the
103 lowest accuracy in reproducing paths), reinforcing the proposed relationship between parahippocampal
104 *theta* oscillations and successful navigation (Bohbot et al., 2017; Chrastil et al., 2022; Jacobs, 2014).
105 These results highlight the potential of using EEG (Event Related Potential and time frequency analyses)
106 to investigate the neural dynamics associated with reorientation impairment in older adults. However,
107 none of these studies considered age-related differences in visuospatial processing despite the
108 considerable impact of age on this cognitive function (Bécu et al., 2023; Segen et al., 2021). Indeed,
109 aging is associated with declines in visual acuity (Faubert, 2002) and a reduced capacity for fine
110 processing which may partially account for navigational impairments in older adults, even more so in
111 environments where visual landmarks are the sole cues for reorientation (Ramanoël et al., 2015, 2020).
112 To address this caveat, the present study aims to examine age-related differences during a landmark-
113 based reorientation task and the associated brain dynamics using EEG recordings from electrodes related
114 to scene-selective brain regions (Harel et al., 2016; Kaiser et al., 2020). In order to investigate the
115 contribution of age-related visuospatial processing declines in reorientation, we manipulated the level
116 of perceptual difficulty, leading to the presentation of large and small landmarks. We hypothesized that
117 older participants would exhibit a poorer navigational performance than young participants, especially
118 when perceptual difficulty is increased (*i.e.*, when landmarks are smaller). At the cortical level, we
119 expected that older adults would show higher parietal P2 amplitude and *theta* activity during
120 reorientation than young adults, reflecting an increased involvement of the scene-selective regions.

121 **2. Methods**

122 **2.1 Participants**

123 We conducted the experiment on a sample population of 30 young participants and 32 healthy older
124 participants. We removed 2 older participants from the analysis because they performed below chance
125 level, and then we cannot ensure their comprehension of the task. In addition, 4 other participants (2
126 older and 2 young participants) were excluded due to excessive artefacts in the EEG data as assessed by
127 signal-to-noise ratio calculation and a careful visual inspection of the signals. Analyses were finally
128 conducted on 28 young participants (mean age: 23.93 years old; SEM = 0.64; range: 19-35; 14 females)
129 and 28 older adults (mean age: 71.25 years old; SEM = 1.01; range: 61–81; 18 females). Participants
130 were right-handed, had no history of neurological or psychiatric disorders and they self-reported normal
131 or corrected-to-normal vision. They were assessed for cognitive impairment using the GRECO French
132 version of the MMSE (Kalafat et al., 2003) with the proposed 26 cut-off to ensure their healthy cognitive
133 status. They also completed a computerized version of the Spatial Orientation Task (Friedman et al.,
134 2020). These results are presented and discussed in the Supplementary Materials (**Table S1**). The
135 experiment was approved by the local Ethical Committee (CERNI-UCA no. 2021-050) and participants
136 provided informed consent before starting the experiment.

137 2.2 Stimuli and procedure

138 Visual stimuli were created using the Unity Engine software (Unity Technologies version 2019.2.0.0f1)
139 and presented on an iiyama ProLiteB2791HSU monitor (1920x1080, 30-83khz) placed at eye level and
140 60 cm away from the participants. Stimuli were presented using the open-source PsychoPy software
141 (v2022.13), implemented on a Dell Precision 7560 computer (Intel® Xeon® W-11955).

142 The environment was adapted from a previous fMRI experiment on healthy aging (Ramanoël et al.,
143 2020). It was a three-arm maze (Y-maze) consisting of three corridors: one branch containing a goal
144 materialized by a gift box, 2 identical starting branches, and 3 three-dimensional (3D) objects positioned
145 at the intersection serving as landmarks (a cube, a ball, and a pyramid). The experimental paradigm was
146 divided into 3 tasks: learning, reorientation, and control (**Figure 1**). During the learning task, participants
147 were passively moved through the maze at 2.5 virtual meter per second, with a rotation speed of 40
148 rad/s. They were instructed to memorize the path to the goal using the objects positioned at the
149 intersection. Then, during the reorientation task, participants were presented with images of the
150 intersection taken from the videos, and they were instructed to indicate the direction of the goal, as
151 quickly and accurately as possible using their right hand to press the directional keys (left or right).
152 These snapshots were extracted from either a near (at 4.25 virtual meters from the intersection) or a far
153 perspective (at 11.2 virtual meters from the intersection) to modulate perceptual difficulty (hereafter
154 referred to as *large* and *small* conditions, respectively). The average retinal visual angle of the landmarks
155 in the small condition was 1.2°, while it was 2.5° in the large condition. Images were presented in a
156 pseudo-randomized order (*i.e.*, a similar stimulus was presented no more than three times in a row) for
157 3 seconds each and were followed by auditory feedback depending on the correctness of the answer
158 given. Afterwards, participants performed the control task which consisted of passively viewing images
159 of the intersection, but this time with all 3 objects being identical (3 spheres, 3 cubes or 3 pyramids).
160 They were instructed to look carefully at both the objects and the fixation cross presented between the
161 different images. To mitigate the possibility of participants losing interest, we varied some properties of
162 the environment (*i.e.*, wall texture and goal location), leading to the presentation of 15 different
163 combinations, presented pseudo-randomly across participants. This sequence of learning, reorientation
164 and control tasks was repeated 3 times for a total of 60 videos, 300 reorientation trials and 180 control
165 trials, and a total acquisition time of 49 minutes.

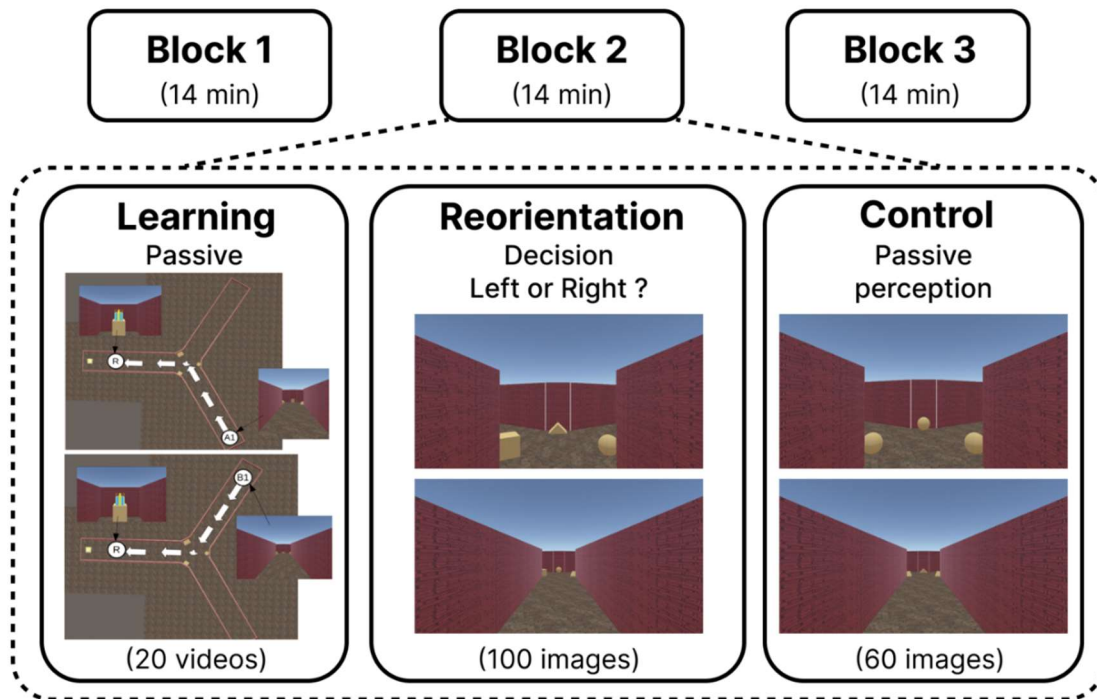


Figure 1. Presentation of the paradigm and some of the stimuli used. Blocks were the same between participants but were presented in a randomized order, with different wall textures. A short break was proposed to all participants between blocks

166 2.3 Recording and Analysis

167 2.3.1 EEG recording and preprocessing

168 EEG was sampled at 500 Hz from 64 Ag/AgCl electrodes mounted in a cap (Waveguard™ original)
169 connected to an amplifier (eego™ mylab, ANT Neuro) and digitized at 24-bit resolution. Data were
170 referenced to CPz electrode, with AFz as ground. Electrode impedances were reduced to at least 20 kΩ,
171 with most values falling below 10 kΩ. Synchronization of EEG recording, and stimulus presentation
172 was ensured by the LabStreamingLayer software Labrecorder (LSL Labrecorder version 1.13). Offline
173 preprocessing was performed with MATLAB (R2021a; The MathWorks Inc., Natick, MA, USA) using
174 custom scripts based on the EEGLAB toolbox version 14.1.0b (Delorme & Makeig, 2004) and adapted
175 from a previously used processing pipeline (Delaux et al., 2021).

176 We first downsampled the data to 250 Hz and corrected the time points for the software delay using the
177 trigger time added to a fixed delay of 50ms for the hardware delay. We automatically removed line noise
178 using the recently developed Zapline-Plus algorithm (Klug & Kloosterman, 2022). We then
179 automatically identified and rejected noisy channels, using the default parameters proposed in the PREP
180 pipeline (Bigdely-Shamlo et al., 2015). On average, 4.25 channels were rejected (SEM= 0.39). These
181 channels were then reconstructed by spherical interpolation of neighboring channels, and the data were
182 re-referenced to the common average. Artifacts were automatically rejected using Artifact Subspace
183 Reconstruction (ASR) (Kothe & Jung, 2015) which uses clean portions of the data to determine
184 thresholds for rejecting components. We used an ASR cutoff parameter of 20, corresponding to the

185 proposed optimal range between 10 and 100 (Chang et al., 2020). We then temporally high-passed the
186 cleaned dataset using a 1.5 Hz Finite Impulse Response (FIR) filter with a Hamming window (with 0.5
187 Hz transition bandwidth, 1.25 Hz passband edge, and 1650 order) (Klug & Gramann, 2021) before
188 applying independent component analysis (ICA) using the Adaptive Mixture Independent Component
189 Analysis (AMICA) algorithm (Palmer et al., 2008). Next, each independent component (IC) was
190 assigned a dipolar source reconstructed with the equivalent dipole model (DipFit ; Oostenveld &
191 Oostendorp, 2002). We used the ICLabel algorithm (Pion-Tonachini et al., 2019) to classify components
192 into 7 classes, using default percentages for classification. We opted for a conservative approach and on
193 average, we retained 14.64 components (SEM = 0.67) corresponding to brain activity. Next, we applied
194 a bandpass filter to the data, with a lower cutoff frequency of 0.3 Hz (with 0.5 Hz transition bandwidth,
195 0.55 Hz passband edge, and 1650 order) to remove slow drifts, and an upper cutoff frequency of 80 Hz
196 (20 Hz transition bandwidth, 80 Hz passband edge, and 42 order) to attenuate high-frequency noise and
197 muscle artifacts. Finally, the preprocessed data were segmented into epochs ranging from -200 ms before
198 to 600 ms after stimulus onset for all conditions. Epochs were excluded from the analysis if less than
199 90% of the period was clean. On average, we kept 76.56% of the epochs (mean epochs kept per subject:
200 367.50; SEM = 2.60). The number of epochs extracted was the same for both age groups ($t_{(1,43.33)} =$
201 0.820, $p = 0.417$).

202 *2.3.2 Event Related Potential and time-frequency analyses*

203 Analyses were restricted to the occipito-parietal electrodes previously associated with scene-selective
204 regions (Harel et al., 2016; Kaiser et al., 2020), corresponding to P6-P8-PO8 for the right hemisphere
205 and P5-P7-PO7 for the left hemisphere. Further data analysis was performed using custom MATLAB
206 scripts with functions from the Fieldtrip toolbox (Oostenveld et al., 2011).

207 For the Event Related Potentials (ERPs), the baseline was identified from -200 ms to image onset
208 corresponding to the recommended minimum of 10 to 20% total epoch length (Luck, 2014), and mean
209 baseline activity was subtracted from the data. Peak amplitude was calculated using the mean amplitude,
210 corresponding to the average of the most positive value surrounded by two lower values. Given the
211 reported effect of aging on peak latency (Kropotov et al., 2016; Mueller et al., 2008), we decided to
212 calculate P1, N1, and P2 latency for each age group. Then, we took a 100 ms wide window around this
213 value to extract the latencies and amplitudes of the individual components.

214 Time-frequency analysis was performed using the superlet approach (Moca et al., 2021), a spectral
215 estimator that uses sets of increasingly constrained bandwidth wavelets to achieve time-frequency super-
216 resolution. For this purpose, we used the Fieldtrip function `ft_freqanalysis` to decompose between 1 and
217 80 Hz, using a width of 2 and a Gaussian width of 3, with an increasing order scaling from 1 to 80. Once
218 the decomposition was completed, we computed event-related spectral perturbations (ERSPs) (Makeig,
219 1993). We used the decibel conversion to normalize power values with a baseline between -250 and -50
220 ms due to temporal smearing (see Cohen, 2014 for more details).

221 2.3.3 Statistical analysis

222 For the ERSs, we performed a non-parametric cluster-based permutation test using a Monte-Carlo
223 estimate to deal with the multiple comparisons problem (Maris & Oostenveld, 2007). We chose the
224 most robust and least conservative method among several modalities, which involved 10 000
225 permutations with weighted cluster mass (Hayasaka & Nichols, 2004) and a cluster-level *alpha* of 0.005
226 to account for multiple comparisons. All other statistical analyses were performed using R Statistical
227 Software (version 4.2.1, R Foundation for Statistical Computing, Vienna, Austria) with R studio
228 (version 2022.07.02+576). After comparing different models using the Akaike information criterion
229 (Akaike, 1974), we decided to use the linear mixed model from the lme4 R package (Bates et al., 2014),
230 with participants included as random intercept. Then, we used the anova function to compute a type III
231 Analysis of Variance (ANOVA) using Satterthwaite's method. The reported results are estimated
232 marginal means computed with the emmeans package in R, using a type III sum of squares, and finally
233 post-hoc Tukey's Honest Significant Difference tests were performed. To ensure normality of residuals
234 and homoscedasticity, both were carefully visually inspected using quantile-quantile plots and boxplots,
235 respectively. Finally, we conducted correlation analyses between ERP peaks and behavioral data using
236 the Bonferroni correction to account for multiple comparisons.

237 **3. Results**

238 3.1 Behavioral results

239 We observed age-related differences in navigation performance. In terms of accuracy (**Figure 2.A**), we
240 reported only a main effect of age ($F_{(1,54)} = 6.63$, $p = 0.013$, $\eta_p^2 = 0.11$, 95% CI = [0.00, 0.28]), with
241 lower accuracy for older adults ($M = 93.4\%$, $SE = 0.94$) compared to young adults ($M = 96.8\%$, $SE =$
242 0.94). There was neither an effect of condition ($F_{(1,54)} = 0.527$, $p > 0.47$) nor an interaction between the
243 factors ($F_{(1,54)} = 0.136$, $p > 0.71$). Regarding the reaction time (**Figure 2.B**), we found a main effect of
244 age ($F_{(1,54)} = 40.97$, $p < 0.001$, $\eta_p^2 = 0.43$, 95% CI = [0.24, 0.58]) in older adults ($M = 1162$ ms, $SE =$
245 35.2) who had a longer reaction time than young adults ($M = 843$ ms, $SE = 35.2$). We also found a main
246 effect of condition ($F_{(1,54)} = 52.47$, $p < 0.001$, $\eta_p^2 = 0.48$, 95% CI = [0.30, 0.63]) with a higher reaction
247 time for the small condition ($M = 1020$ ms, $SE = 25$) compared to the large condition ($M = 985$ ms, SE
248 $= 25$) for both young and older adults. There was no interaction between age and condition ($F_{(1,54)} =$
249 1.48 , $p = 0.229$).

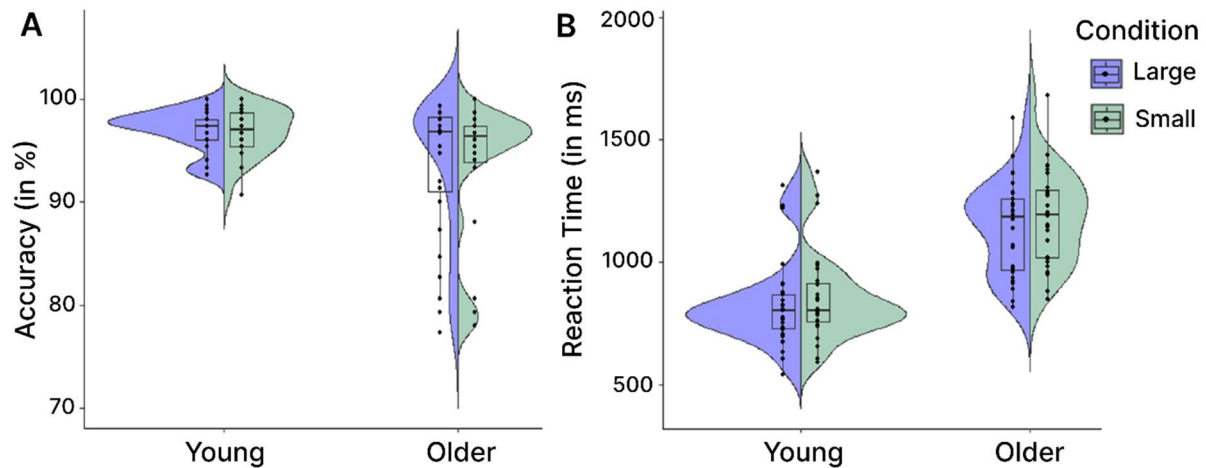


Figure 2. Performance of participants in the reorientation task. Individual points represent the average for each participant. **A.** Accuracy computed as the percentage of reorientation errors over all trials. **B.** Reaction time between the presentation of the stimulus and the recorded response.

250 3.2 ERPs results for large and small conditions during reorientation

251 In this analysis we compared the large and small conditions to examine the effect of age with perceptual
252 difficulty during the reorientation task (**Figure 3**).

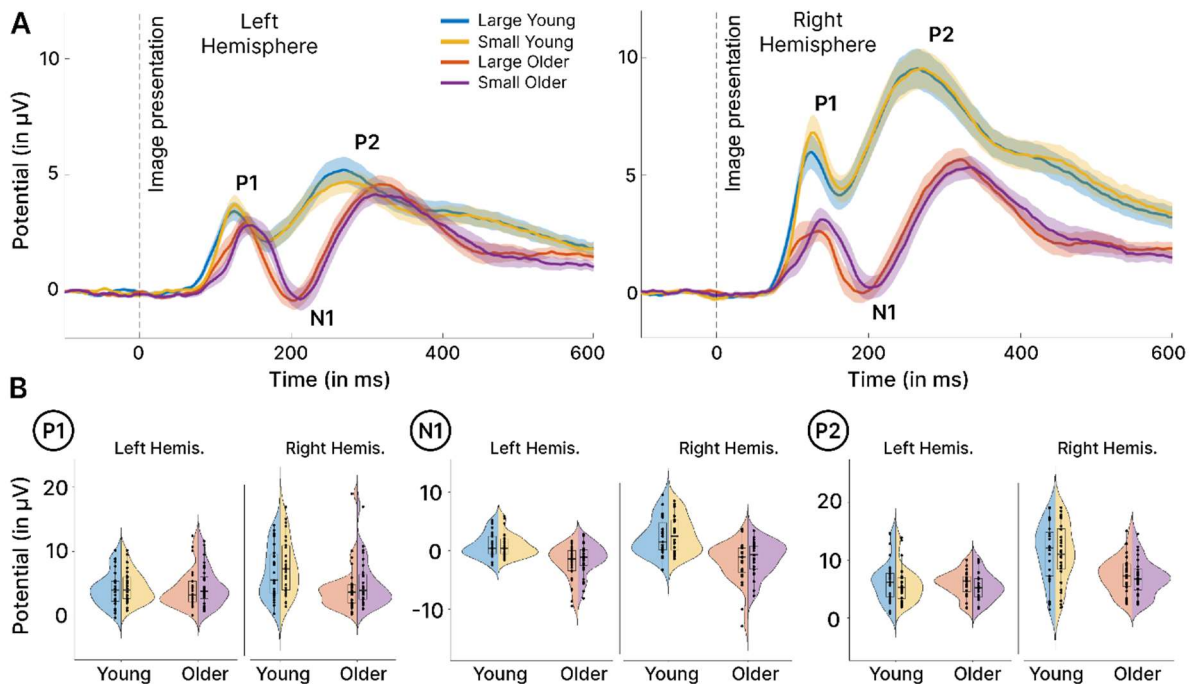
253 *P1, N1, and P2 amplitudes*

254 First, we evaluated the age effect by comparing the EEG recordings of young and older adults. We found
255 no main effect of age for P1 amplitude ($F_{(1,54.17)} = 2.57, p = 0.11$), but a higher amplitude for young than
256 older adults when considering only the right hemisphere ($t_{(67)} = 3.02, p = 0.018, d = 1.29, 95\% \text{ CI} =$
257 $[0.43, 2.15]$). We reported an increased N1 amplitude (*i.e.*, more negative) for older adults compared to
258 young adults ($F_{(1,54.09)} = 28.92, p < 0.001, \eta_p^2 = 0.35, 95\% \text{ CI} = [0.16, 0.51]$) in both hemispheres. We
259 also observed a lower P2 amplitude in older adults compared to young adults ($F_{(1,54)} = 7.36, p < 0.001,$
260 $\eta_p^2 = 0.12, 95\% \text{ CI} = [0.01, 0.29]$) but this age effect was restricted to the right hemisphere ($t_{(68)} = 4.58,$
261 $p < 0.001, d = 1.82, 95\% \text{ CI} = [-1.00, 2.62]$), with no difference for the left hemisphere ($t_{(68.3)} = 0.53, p$
262 $= 0.95$).

263 Next, we considered the effect of condition comparing large *vs.* small. We found a higher P1 amplitude
264 for the small condition compared to the large condition ($F_{(1,159.25)} = 4.91, p = 0.028, \eta_p^2 = 0.03, 95\% \text{ CI}$
265 $= [0.00, 0.10]$). There was no modulation of either N1 ($F_{(1,159)} = 3.43, p = 0.066$), or P2 amplitudes
266 ($F_{(1,162)} = 1.70, p = 0.19$).

267 Finally, we examined the lateralization effect by directly comparing the brain signals from the right and
268 left hemispheres. We reported a higher amplitude for P1 in the right hemisphere ($F_{(1,159.77)} = 33.74, p <$
269 $0.001, \eta_p^2 = 0.17, 95\% \text{ CI} = [0.08, 0.28]$), but this effect was restricted to young adults, as older adults
270 showed no lateralization ($t_{(159)} = 0.76, p = 0.87$). For P2, we found a higher amplitude in the right
271 hemisphere independent of age group ($F_{(1,162)} = 122.29, p < 0.001, \eta_p^2 = 0.43, 95\% \text{ CI} = [0.32, 0.52]$).
272 Considering N1, we observed the opposite, with a greater amplitude in the left hemisphere ($F_{(1,159.79)} =$

273 15.15, $p < 0.001$, $\eta_p^2 = 0.09$, 95% CI = [0.02, 0.18]). This effect was restricted to young adults ($t_{(160)} =$
 274 5.13, $p < 0.001$, $d = 0.99$, 95% CI = [0.60, 1.39]), whereas older adults presented similar N1 activity for
 275 both hemispheres ($t_{(159)} = 0.32$, $p = 0.99$).



276

Figure 3. ERP results for near and far conditions during the reorientation task. **A.** Grand-average ERPs considering age (young/older), condition (large/small) and hemisphere (left/right) as variables, individually baselined corrected. Activity averaged over P6-P8-PO8 electrodes for the right hemisphere and over P5-P7-PO7 electrodes for the left hemisphere. **B.** Split violin plot of extracted individual amplitudes for P1, N1 and P2 component. Statistics were computed using these values.

277

278 ***P1, N1, and P2 latencies***

279 Looking at the age effect, we found later peaks for older adults in P1 ($F_{(1,54.35)} = 13.12$, $p < 0.001$, $\eta_p^2 =$
 280 0.19, 95 % CI = [0.04, 0.37]), N1 ($F_{(1,53.92)} = 37.24$, $p < 0.001$, $\eta_p^2 = 0.41$, 95 % CI = [0.21, 0.56]) and
 281 P2 ($F_{(1,54)} = 130.25$, $p < 0.001$, $\eta_p^2 = 0.71$, 95% CI = [0.57, 0.79]). The effect for P1 was restricted to the
 282 small condition ($t_{(77)} = 4.76$, $p < 0.001$, $d = 1.57$, 95% CI = [0.90, 2.24]) as we reported no age difference
 283 for the large condition ($t_{(77)} = 1.85$, $p = 0.26$).

284 Considering the condition effect, we observed a delayed P1 for the small condition compared to the
 285 large condition ($F_{(1,159.53)} = 20.89$, $p < 0.001$, $\eta_p^2 = 0.12$, 95% CI = [0.04, 0.21]). This effect was not
 286 present for either N1 ($F_{(1,159.28)} = 1.85$, $p = 0.544$), or P2 ($F_{(1,162)} = 1.52$, $p = 0.22$). This condition effect
 287 for P1 was present only for older adults ($t_{(159)} = 5.80$, $p < 0.001$, $d = 1.10$, 95% CI = [0.71, 1.49]) with
 288 no difference for young adults ($t_{(159)} = 0.70$, $p = 0.90$).

289 Finally, concerning lateralization, we found no effect for P1 ($F_{(1,160.32)} = 3.76, p = 0.054$) or N1 ($F_{(1,160.41)}$
290 $= 3.64, p = 0.058$). For P2, we observed a later peak in the right hemisphere compared to the left
291 hemisphere ($F_{(1,162)} = 4.14, p = 0.043, \eta_p^2 = 0.03, 95\% \text{ CI} = [0.00, 0.54]$).

292 *3.3 ERP results comparing reorientation and control tasks*

293 In this second analysis, we compared the activity elicited by the reorientation task and the control task,
294 in order to dissociate reorientation from pure scene perception effects. The results presented below
295 correspond to the large and small conditions merged together (**Figure 4**). Before doing so, we checked
296 that the same pattern of results was obtained when the two conditions were considered separately.

297 *P1, N1 and P2 Amplitudes*

298 First, we examined the age effect, comparing young and older adults. We found no effect for P1
299 amplitude ($F_{(1,54.06)} = 2.15, p = 0.15$), but a higher amplitude for young adults when considering the right
300 hemisphere only ($t_{(68)} = 2.99, p = 0.019, d = 1.21, 95\% \text{ CI} = [0.39, 2.02]$), with no age difference in the
301 left hemisphere ($t_{(67.6)} = 0.23, p = 0.996$). We found a higher N1 amplitude (*i.e.*, more negative) for older
302 adults ($F_{(1,54.08)} = 31.82, p < 0.001, \eta_p^2 = 0.37, 95\% \text{ CI} = [0.18, 0.53]$), and the opposite pattern for P2,
303 with a higher amplitude for young adults ($F_{(1,84)} = 10.33, p = 0.002, \eta_p^2 = 0.16, 95\% \text{ CI} = [0.02, 0.34]$).

304 We then considered the task and compared reorientation and control (*i.e.*, passive perception). We found
305 a similar pattern, with a higher amplitude for the reorientation task for P1 ($F_{(1,161.14)} = 4.32, p = 0.040,$
306 $\eta_p^2 = 0.03, 95\% \text{ CI} = [0.00, 0.09]$), N1 ($F_{(1,161.16)} = 13.90, p < 0.001, \eta_p^2 = 0.08, 95\% \text{ CI} = [0.02, 0.17]$)
307 and P2 ($F_{(1,162)} = 44.38, p < 0.001, \eta_p^2 = 0.22, 95\% \text{ CI} = [0.11, 0.32]$). Considering only N1 amplitude,
308 the effect was limited to older adults ($t_{(159)} = 3.98, p < 0.001, d = 0.75, 95\% \text{ CI} = [0.37, 1.14]$), as young
309 adults showed no difference between reorientation and control for this component ($t_{(161)} = 1.30, p =$
310 0.57).

311 Finally, we considered lateralization, comparing the left and right hemispheres. We reported a similar
312 pattern for positive components, with a higher amplitude in the right hemisphere for P1 ($F_{(1,161.14)} =$
313 $32.22, p < 0.001, \eta_p^2 = 0.17, 95\% \text{ CI} = [0.07, 0.27]$) and P2 ($F_{(1,162)} = 95.95, p < 0.001, \eta_p^2 = 0.37, 95\%$
314 $\text{CI} = [0.26, 0.47]$). These results were only observed for young adults, as older adults showed no
315 lateralization effect for either the P1 ($t_{(161)} = 0.58, p = 0.94$) or the P2 component ($t_{(162)} = 2.43, p = 0.12$).
316 For N1, we found the opposite result, with a higher amplitude for the left hemisphere ($F_{(1,161.16)} = 14.83,$
317 $p < 0.001, \eta_p^2 = 0.08, 95\% \text{ CI} = [0.02, 0.18]$), again only for young adults ($t_{(159)} = 5.94, p < 0.001, d =$
318 $1.13, 95\% \text{ CI} = [0.73, 1.52]$) with no lateralization for older adults ($t_{(161)} = 0.51, p = 0.96$).

319 *P1, N1 and P2 Latencies*

320 First, we observed a similar pattern for age differences across components, with a later peak for P1
321 ($F_{(1,54.06)} = 12.12, p < 0.001, \eta_p^2 = 0.18, 95\% \text{ CI} = [0.04, 0.36]$), N1 ($F_{(1,53.87)} = 47.88, p < 0.001, \eta_p^2 =$
322 $0.47, 95\% \text{ CI} = [0.28, 0.61]$) and P2 ($F_{(1,54)} = 154.14, p < 0.001, \eta_p^2 = 0.74, 95\% \text{ CI} = [0.62, 0.82]$). The
323 age difference for P1 was present in the left hemisphere only ($t_{(69.8)} = 4.16, p < 0.001, d = 1.58, 95\% \text{ CI}$

324 = [0.81, 2.35]), as we reported no age-related modulation of P1 for the right hemisphere ($t_{(70)} = 2.36$, p
 325 = 0.10).

326 When comparing reorientation and control tasks, there was no difference in P1 latency ($F_{(1,161.15)} = 0.08$,
 327 $p = 0.77$). We observed a similar pattern for the other two components, with a later peak for the
 328 reorientation task for N1 ($F_{(1,161.01)} = 9.34$, $p = 0.003$, $\eta_p^2 = 0.05$, 95% CI = [0.01, 0.14]) and P2 ($F_{(1,162)}$
 329 = 58.59, $p < 0.001$, $\eta_p^2 = 0.27$, 95% CI = [0.16, 0.37]).

330 For lateralization, comparing left and right hemispheres, we observed a later P1 peak for the left
 331 hemisphere ($F_{(1,161.15)} = 4.96$, $p = 0.027$, $\eta_p^2 = 0.03$, 95% CI = [0.00, 0.10]), with a similar pattern for the
 332 N1 component ($F_{(1,161.01)} = 6.31$, $p = 0.013$, $\eta_p^2 = 0.04$, 95% CI = [0.00, 0.11]). Considering P2, we found
 333 no difference between the left and right hemispheres ($F_{(1,162)} = 1.17$, $p = 0.28$). The later P1 peak was
 334 observed for older adults only ($t_{(161.2)} = 3.39$, $p = 0.005$, $d = 0.64$, 95% CI = [0.26, 1.02]).

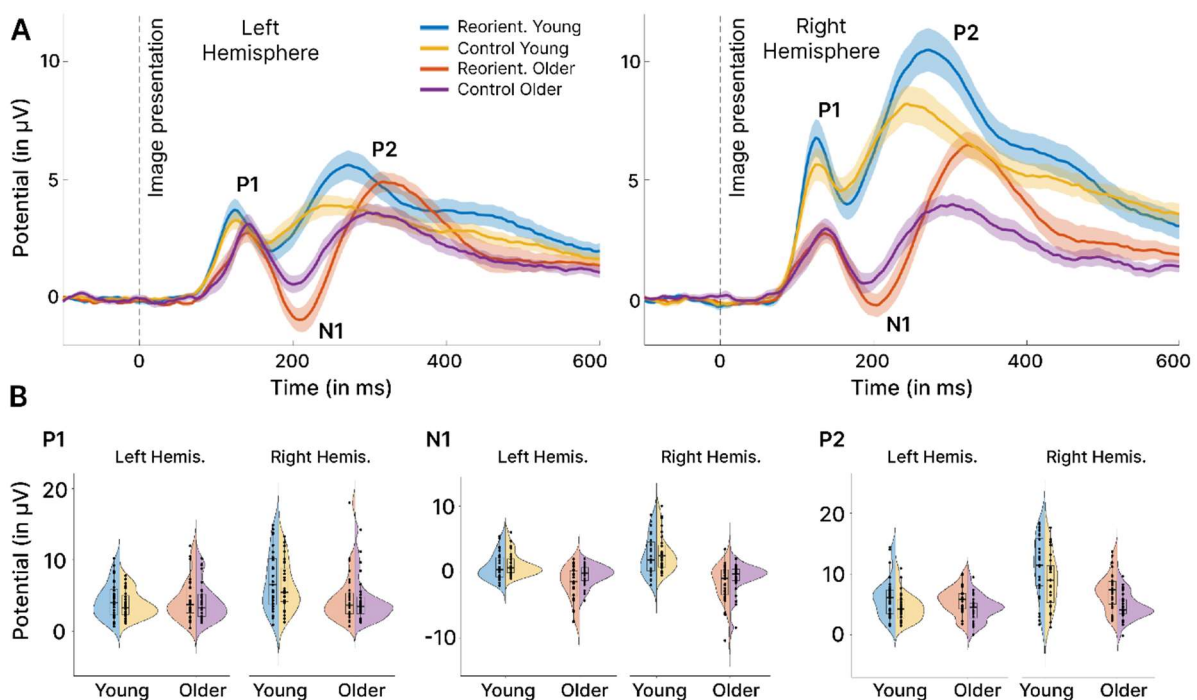
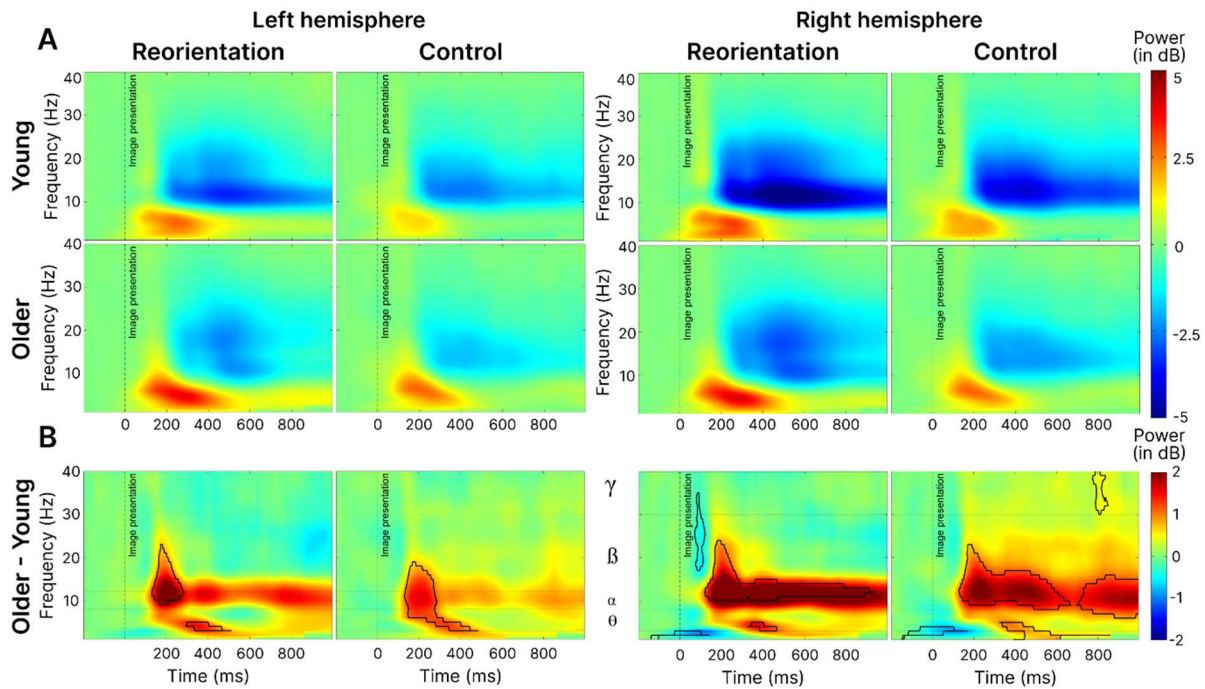


Figure 4. ERP results comparing reorientation and control tasks. **A.** Grand-average ERPs considering age (young/older), task (reorientation/control) and hemisphere (left/right) as variables, individually baselined corrected. Activity averaged over P6-P8-PO8 electrodes for the right hemisphere and over P5-P7-PO7 electrodes for the left hemisphere. **B.** Split violin plot of extracted individual amplitudes for P1, N1 and P2 components. Statistics were computed using these values.

335 3.4 ERSP results comparing reorientation and control tasks

336 Finally, we examined brain oscillations by computing ERSP. This allowed us to examine additional
 337 information about the underlying cognitive process beyond ERPs (Herrmann et al., 2014).



338

Figure 5. ERSP results comparing reorientation and control tasks. **A.** Grand-average ERSPs, considering age (young/older), task (reorientation/control) and hemisphere (left/right) as variables, using decibel baseline (-150 to -50 ms) normalization. Activity averaged over P6-P8-PO8 electrodes for the right hemisphere and over P5-P7-PO7 electrodes for the left hemisphere. **B.** ERSP activity of older minus young adults. The black line corresponds to cluster-based permutation tests results with p-value < 0.05.

339 For all ERSP analyses (**Figure 5.A.**), we found a similar pattern consisting of an increased
 340 synchronization (*i.e.*, an increase in power interpreted as an increase in neural firing synchronization of
 341 the underlying neuronal population compared to the selected baseline) in low frequency bands,
 342 *delta/theta* (1-8 Hz), occurring 50 ms before image presentation for young adults and lasting up to +400
 343 ms and up to +500 ms for older adults in the reorientation task. This synchronization was followed by
 344 desynchronization in the higher frequency bands *alpha* (8-13 Hz) and *beta* (13-30 Hz). We then
 345 conducted a cluster-based permutation tests on these results (**Figure 5.B.**). In the right hemisphere, we
 346 reported a decreased synchronization in the *alpha/beta* band in older adults compared to young adults,
 347 starting from +200 ms and lasting until +1000 ms. In the left hemisphere, this result was significant only
 348 within a short window around +200 ms. We also reported a decreased synchronization in the *delta* (1-3
 349 Hz) band for older adults compared to their younger counterparts, starting from 50 ms before image
 350 presentation up to +200 ms. Older adults also showed an increase in *theta* (3-8 Hz) synchronization,
 351 with a burst starting just after +200 ms and lasting up to +400 ms, and a decrease in high *beta* band
 352 synchronization for the reorientation task specific to the right hemisphere.

353 3.5 Correlation analyses between ERP and Behavioral data

354 We performed correlational analyses between ERP (peak amplitudes and latencies) and behavioral data
 355 (reaction times and accuracies), separately for young and older adults. This resulted in a total of 48

356 comparisons, with no significant results after Bonferroni correction. A table with all the uncorrected p -
357 values is available in the Supplementary Materials (Table S2).

358 **4. Discussion**

359 This EEG study aimed to investigate age-related differences during a landmark-based reorientation task
360 and their neural correlates. Consistent with previous studies, our results indicate that older adults
361 demonstrate reduced navigational abilities, as evidenced by slower and less precise reorientation.
362 However, in contrast with our initial hypothesis, the perception of landmarks of different sizes was not
363 a deteriorating factor for older adults' performance on the task, even though it was associated with a
364 delayed P1 component in older adults only. Age-related reorientation deficits were associated with
365 differences in the neural dynamics of high-level visual processing. Indeed, we found delayed latencies
366 of the P1, N1 and P2 components recorded from occipito-parietal electrodes associated with scene-
367 selective regions. Moreover, older adults displayed decreased P1 and P2 amplitudes as well as lower
368 *alpha/beta* desynchronization in the right hemisphere specifically. Finally, only older adults exhibited
369 increased N1 amplitude in both hemispheres for the reorientation task, accompanied by higher levels of
370 *theta* power. These results points toward a three-part process that may contribute to older adults'
371 difficulties in landmark reorientation, involving slower and less efficient visual processing, more
372 effortful processing of visuospatial information, and a deficit in the attentional mechanism related to the
373 selection of task-relevant stimuli.

374 ***Reorientation performance is impaired in aging and reaction time decreases similarly for both age*** 375 ***groups when perceptual difficulty increases***

376 The behavioral results indicated that young adults performed better, with a lower reaction time and a
377 higher rate of recovered paths. These results support previous findings that older adults are impaired
378 during a navigation task which solely relies on the use of visual landmarks for reorientation (Bécu et al.,
379 2023; West et al., 2023). It is worth mentioning, that despite their diminished performance, older adults
380 still achieved a high level of accuracy which may be explained by the relative simplicity of the task and
381 their healthy cognitive status. Increasing perceptual difficulty (*i.e.*, decreasing landmark size) did not
382 increase error rate, but it did lead to an increase in reaction time in both age groups. This finding is
383 consistent with the well-characterized relationship between stimulus size and reaction time (Plewan &
384 Rinkenauer, 2017; Sperandio et al., 2009). However, contrary to our hypotheses, older adults did not
385 show greater difficulty than young adults when perceptual difficulty was manipulated. This lack of
386 behavioral difference is in line with our EEG findings, which showed no interaction effect between
387 perceptual difficulty and age; both age groups displayed a similar increase in P1 amplitude in the small
388 landmark condition. However, we reported a later P1 peak amplitude only for older adults in the small
389 condition compared to the large condition. It has been suggested that the P1 component is modulated by
390 visuospatial attention (Di Russo et al., 2003), but the exact functional basis of this effect remains

391 debated. The “P1 inhibition-timing” model proposed by Klimesch et al. (2007, 2011) suggests that the
392 P1 reflects a transient inhibitory filter that operates to increase the signal-to-noise ratio allowing an
393 efficient early categorization process. This component may be the earliest index of attentional control,
394 being increased over posterior regions when processing complexity is high (Fellinger et al., 2012).
395 Moreover, the fact that older adults presented a decreased P1 amplitude suggests that they may have
396 impairments in the early categorization process of visual stimuli which are exacerbated by the
397 reorientation task. Then, when faced with increased perceptual difficulty older adults required more time
398 to allocate greater attentional resources to the harder perceptual task (Sawetsuttipan et al., 2023). These
399 findings align with the two leading cognitive aging hypotheses which posit that aging is associated with
400 an inhibitory deficit (*i.e.*, decreased P1 amplitude) and the processing speed hypothesis, (*i.e.*, increased
401 P1 latency) when the perceptual difficulty of the task is increased (Finnigan et al., 2011; Gazzaley et al.,
402 2008). It is worth noting that although there was a difference in P1 latency, neither age-related
403 modulation was observed for the later components (namely, N1 and P2) nor for behavioral data. This
404 suggests that the delay in P1 latency may not significantly affect performance with a possible later
405 mechanism compensating for this early delay.

406 ***N1 amplitude and theta power reflects increased resources allocation for landmark processing by*** 407 ***older adults***

408 Regarding the N1 component, we observed that older adults exhibited an increased amplitude in both
409 hemispheres compared to young adults. Additionally, we found that older adults had a higher N1
410 amplitude during the reorientation phase than during passive perception, and that this pattern was not
411 observed in young adults. Some authors have suggested that the N1 component reflect enhanced visual
412 information processing (Luck, 1995; Vogel & Luck, 2000) and visual stimuli discrimination (Finnigan
413 et al., 2011; Hillyard et al., 1998; Hopf et al., 2002; Warbrick et al., 2014; Wiegand et al., 2014). The
414 N1 was previously associated with the activity of the posterior precuneus (Natale et al., 2006). This
415 region plays a role in allocating attention to spatial information, encoding and retrieving spatial
416 memories, and identifying and using relevant landmarks (Cona & Scarpazza, 2019; Delaux et al., 2021).
417 Intracranial EEG recordings also pointed out the activity of the precuneus activity occurring around
418 210ms after the presentation of a stimulus, while also highlighting the activity of the PPA around 170ms
419 (Bastin et al., 2013; Vlcek et al., 2020). During the same time window as the N1 component, we also
420 observed an increase in *theta* activity. The link between *theta* power and the N1 component was
421 proposed by Klimesch et al. (2004) arguing that the power in the N1 time window was generated
422 primarily by frequencies in the *theta* range (Gruber et al., 2005; Van der Lubbe et al., 2016). Here, we
423 observed an increased *theta* synchronization during the reorientation task, which was more pronounced
424 in older adults, with a burst occurring after 200ms. This increase in *theta* activity was also observed by
425 Lithfous et al. (2018) during a maze reorientation task and associated with better performance in the
426 older group. They interpreted their results as a possible compensatory mechanism exhibited by high-

427 performing older adults, which highlights the importance of parietal *theta* activity for a successful
428 visually-guided navigation (Chrastil et al., 2022). Taken together our results emphasize the role of the
429 N1 component in landmark-based spatial navigation in the context of aging. They provide evidence for
430 an increased bilateral activity in the *theta* band on electrodes associated with scene-selective regions
431 suggesting that older adults resort to more extensive neural resources to process visual landmarks.

432 ***Age-related decrements in selective attention during task-relevant information processing***

433 Regarding the P2 component, we found that older adults exhibited a reduced amplitude compared to
434 younger adults. Conversely, we observed a similar enhancement of amplitude in both age groups when
435 they performed the reorientation task versus the passive perception. These results seem to indicate that
436 the age-related decrease in P2 amplitude reflects a general impairment in the capacity to complete a
437 visual discrimination task, regardless of the reorientation task. The literature has proposed that this
438 posterior P2 component may reflect the mediation of information between memory systems, as a way
439 to compare visual inputs and information stored in the working memory (Cepeda-Freyre et al., 2020;
440 Freunberger et al., 2007; Lefebvre et al., 2005). Other recent findings suggest that the P2 component
441 may rather represent a top-down attentional control during visual processing of objects (Lai et al., 2020),
442 indicating enhanced selective attention by task-relevant stimulus (Freunberger et al., 2007; Mecklinger
443 et al., 2009; Philips & Takeda, 2009). As we observed a similar age-related decrease in a task that did
444 not involve working memory (*i.e.*, a passive perception), we argue that the P2 amplitude decrease we
445 report may reflect the well-supported age-related decline in top-down selection of task-relevant objects,
446 which are the landmarks in our case (Lai et al., 2020). However, we cannot exclude that this decrease
447 in P2 amplitude among older adults could also be ascribed to the decline in spatial working memory due
448 to cognitive aging as reported in previous studies (Finnigan et al., 2011; Kléncklen et al., 2012). This
449 proposed age-related decrease in spatial information processing is also supported by our ERSP results,
450 showing a decrease of *alpha/beta* desynchronization among older adults. It has been suggested that these
451 frequency bands support the endogenous activation of neuronal ensembles involved in task-relevant
452 information processing (Griffiths et al., 2019; Hanslmayr et al., 2012; Spitzer & Haegens, 2017). They
453 were also previously observed during good reorientation choices in spatial navigation task (Chrastil et
454 al., 2022), interpreted as the reflect of memory retrieval process (Klimesch, 1997, 1999). Finally, we
455 hypothesized an increase in P2 amplitude with aging, in light of the findings from Ramanoël et al. (2020)
456 who reported an increase in OPA activity among older adults during active reorientation, the OPA
457 activity proposed to be reflected in the parietal P2 component (Harel et al., 2016, 2022; Kaiser et al.,
458 2020). However, in their work, Ramanoël et al. (2020) had subjects actively navigate in the maze, and
459 used fMRI recordings, which have some important differences that may account for the differences we
460 observed. Moreover, the OPA may not be the only scene-selective brain regions contributing to the P2
461 component, and spatial sensitivity of scalp EEG does not allow us to distinguish between OPA and PPA
462 for example. This was suggested by Kaiser et al. (2020) who also reported, along with OPA, activity of

463 the PPA during this time window which was proposed in an iEEG study to last for thousands of
464 milliseconds (Vlcek et al., 2020), possibly overlapping over occipito-parietal electrodes (Persichetti &
465 Dilks, 2019).

466 *Aging decreases lateralization of visuospatial processing*

467 Finally, we found a distinct lateralization of brain activity in young adults, with greater activation
468 observed in the right hemisphere than in the left hemisphere during both the passive perception and
469 reorientation phases of the experiment. Harel et al. (2016, 2022) similarly observed higher amplitudes
470 in the right hemisphere among young adults only, during a passive scene perception task. This is
471 consistent with the commonly accepted notion that selective spatial attention and spatial working
472 memory are controlled by a predominantly right hemisphere network (Awh & Jonides, 2001; Young,
473 2012). This also appears to hold true during human spatial navigation as reported in a meta-analysis of
474 47 fMRI studies (Li et al., 2021). In our results, this lateralization was weaker among older adults for
475 P1 and P2 components, and amplitude was lower in the right hemisphere among older adults only. Using
476 a visuospatial task, Learmonth et al. (2017) also reported decreased right hemisphere control among
477 older adults during a visuospatial task and our results confirm the hypothesis of right hemisphere
478 engagement decrease with age as proposed by the right hemi-aging model (Dolcos et al., 2002). This
479 result also highlights the importance of considering both hemispheres separately when conducting ERP
480 or ERSP investigations of age-related modifications.

481 *Limitations and perspectives*

482 One of the main limitations of our results is that we did not find any correlation between behavioral and
483 EEG data. This can be explained by the relative behavioral simplicity of our task, which may have
484 prevented us from capturing subtle variations in performance. Furthermore, concerning the modulations
485 of the P1, N1, and P2 components, their interpretation in an independent way could be exaggerated as
486 we acknowledge the possibility that effects observed on later peaks may depend on preceding peaks.
487 For instance, it is conceivable that P1 modulations may exert an effect on N1 peak, rendering the
488 conventional label "component" potentially misleading (Luck, 2005).

489 In an effort to disentangle reorientation from passive perception, we introduced a cognitive load
490 disparity between the two tasks, which may account in part for the observed results, particularly for the
491 P2 component. To address this issue, future investigations might consider including control tasks relying
492 on stimulus detection and decision-making paradigms, such as the N-back task. Finally, given the
493 changes in visual exploration between young and older adults and their impact on information
494 processing (Bécu et al., 2020, 2023; Durteste et al., 2023; Ryan et al., 2022) it would be worthwhile to
495 investigate the effect of age on gaze patterns during a landmark-based reorientation task, linking EEG
496 with eye-tracking data to gain more insight into how older adults are impaired in using landmarks during
497 reorientation.

498 **5. Conclusion**

499 Our study aimed to investigate age-related differences in visuospatial processing and the underlying
500 brain dynamics within scene-selective regions in young and healthy older adults performing a landmark-
501 based reorientation task. Older adults showed reduced reorientation performance along with increased
502 latency of early cortical markers of visual processing in scene-selective regions, suggesting that
503 navigational deficits may result from delayed processing of visuospatial information. Decreasing
504 landmark size and thus increasing perceptual difficulty led to a delayed P1 component only in older
505 adults, suggesting an age-related delayed early categorization of smaller landmarks. Our EEG data also
506 revealed a three-part process that may partially account for older adults' challenges during landmark
507 reorientation. First, a delayed and reduced P1 component indicated slower and less efficient visual
508 processing, including stimulus discrimination. Second, the increase in N1 amplitude and theta-band
509 activity indicated a greater demand on cognitive resources, leading to more effortful processing of
510 visuospatial information. Third, the reduction in P2 amplitude associated with *alpha-beta* activity
511 suggested a deficiency in the attentional mechanism for selecting task-relevant stimuli. Finally, our
512 findings underscore the importance of considering both hemispheres separately when studying aging,
513 as they highlight an age-related decrease in right hemisphere specific activity. Taken together, these
514 results highlight the interest of using EEG to gain insight into age-related modulations of neural
515 correlates of visuospatial processing during reorientation, while paving the way for further
516 investigations to better characterize the brain dynamics underlying spatial navigation deficits in healthy
517 older adults.

518 **CRedit author statement**

519 **Naveilhan Clément:** Conceptualization, Methodology, Formal analysis, Investigation, Writing –
520 Original Draft; **Alexandre Delaux:** Conceptualization, Methodology, Writing – Review & Editing;
521 **Marion Durteste:** Conceptualization, Methodology, Writing - Review & Editing; **Jerome Lebrun:**
522 Writing – Review & Editing, Methodology; **Raphaël Zory:** Writing – Review & Editing, Funding
523 acquisition; **Angelo Arleo:** Writing - Review & Editing, Funding acquisition; **Stephen Ramanoël:**
524 Conceptualization, Supervision, Writing – Review & Editing, Funding Acquisition, Project
525 administration.

526 **Disclosure statement**

527 No author involved with this research had any conflicts of interest. This work was approved by the local
528 Ethical Committee of Université Côte d'Azur (CERNI-UCAn°2021-050) and participants provided
529 informed consent before starting the experiment.

530 **Acknowledgements**

531 The authors gratefully acknowledge Maud Saulay-Carret for her help with acquisitions and also the
532 voluntary participants involved in this research.

533 This work was supported by the French government through the UCA^{JEDI} project managed by the
534 National Research Agency (ANR-15- IDEX-01) and, in particular, by the interdisciplinary Institute for
535 Modeling in Neuroscience and Cognition (NeuroMod) of Université Côte d'Azur. It was also supported
536 by the Fondation pour la Recherche sur Alzheimer, the French National Research Agency (ANR-18-
537 CHIN-0002), the LabEx LIFESENSES (ANR-10-LABX-65), and the IHU FOReSIGHT (ANR-18-
538 IAHU-01). The funders had no role in study design, data collection and analysis, decision to publish or
539 preparation of the manuscript.

540 **Code and data availability**

541 All raw data, codes and stimuli generated for the purpose of analyses in this paper are available via the
542 OSF repository: https://osf.io/crne8/?view_only=7a34edf4644e49a796442388ce7ac885

543 **References**

- 544 Akaike, H. (1974). A new look at the statistical model identification. *IEEE Transactions on Automatic*
545 *Control*, 19(6), 716-723. <https://doi.org/10.1109/TAC.1974.1100705>
- 546 Awh, E., & Jonides, J. (2001). Overlapping mechanisms of attention and spatial working memory.
547 *Trends in Cognitive Sciences*, 5(3), 119-126. [https://doi.org/10.1016/S1364-6613\(00\)01593-X](https://doi.org/10.1016/S1364-6613(00)01593-X)
- 548 Barrash, J. (1994). Age-related decline in route learning ability. *Developmental Neuropsychology*,
549 10(3), 189-201. <https://doi.org/10.1080/87565649409540578>
- 550 Bastin, J., Vidal, J. R., Bouvier, S., Perrone-Bertolotti, M., Bénis, D., Kahane, P., David, O., Lachaux,
551 J.-P., & Epstein, R. A. (2013). Temporal Components in the Parahippocampal Place Area
552 Revealed by Human Intracerebral Recordings. *Journal of Neuroscience*, 33(24), 10123-10131.
553 <https://doi.org/10.1523/JNEUROSCI.4646-12.2013>
- 554 Bates, D., Mächler, M., Bolker, B., & Walker, S. (2014). *Fitting Linear Mixed-Effects Models using*
555 *lme4* (arXiv:1406.5823; Version 1). arXiv. <https://doi.org/10.48550/arXiv.1406.5823>
- 556 Bécu, M., Sheynikhovich, D., Ramanoël, S., Tatur, G., Ozier-Lafontaine, A., Authié, C. N., Sahel, J.-
557 A., & Arleo, A. (2023). Landmark-based spatial navigation across the human lifespan. *eLife*,
558 12, e81318. <https://doi.org/10.7554/eLife.81318>
- 559 Bécu, M., Sheynikhovich, D., Tatur, G., Agathos, C. P., Bologna, L. L., Sahel, J.-A., & Arleo, A.
560 (2020). Age-related preference for geometric spatial cues during real-world navigation. *Nature*
561 *Human Behaviour*, 4(1), Article 1. <https://doi.org/10.1038/s41562-019-0718-z>
- 562 Bigdely-Shamlo, N., Mullen, T., Kothe, C., Su, K.-M., & Robbins, K. A. (2015). The PREP pipeline :
563 Standardized preprocessing for large-scale EEG analysis. *Frontiers in Neuroinformatics*, 9,
564 16. <https://doi.org/10.3389/fninf.2015.00016>
- 565 Bohbot, V. D., Copara, M. S., Gotman, J., & Ekstrom, A. D. (2017). Low-frequency theta oscillations
566 in the human hippocampus during real-world and virtual navigation. *Nature Communications*,
567 8, 14415. <https://doi.org/10.1038/ncomms14415>
- 568 Bonner, M. F., & Epstein, R. A. (2017). Coding of navigational affordances in the human visual
569 system. *PNAS Proceedings of the National Academy of Sciences of the United States of*
570 *America*, 114, 4793-4798. <https://doi.org/10.1073/pnas.1618228114>

- 571 Burns, P. C. (1999). Navigation and the mobility of older drivers. *The Journals of Gerontology. Series*
572 *B, Psychological Sciences and Social Sciences*, 54(1), S49-55.
573 <https://doi.org/10.1093/geronb/54b.1.s49>
- 574 Cepeda-Freyre, H. A., Garcia-Aguilar, G., Eguibar, J. R., & Cortes, C. (2020). Brain Processing of
575 Complex Geometric Forms in a Visual Memory Task Increases P2 Amplitude. *Brain Sciences*,
576 10(2), 114. <https://doi.org/10.3390/brainsci10020114>
- 577 Chang, C.-Y., Hsu, S.-H., Pion-Tonachini, L., & Jung, T.-P. (2020). Evaluation of Artifact Subspace
578 Reconstruction for Automatic Artifact Components Removal in Multi-Channel EEG
579 Recordings. *IEEE Transactions on Biomedical Engineering*, 67(4), 1114-1121.
580 <https://doi.org/10.1109/TBME.2019.2930186>
- 581 Chrastil, E. R., Rice, C., Goncalves, M., Moore, K. N., Wynn, S. C., Stern, C. E., & Nyhus, E. (2022).
582 Theta oscillations support active exploration in human spatial navigation. *NeuroImage*, 262,
583 119581. <https://doi.org/10.1016/j.neuroimage.2022.119581>
- 584 Cohen, M. X. (2014). *Analyzing Neural Time Series Data : Theory and Practice*. MIT Press.
- 585 Cona, G., & Scarpazza, C. (2019). Where is the « where » in the brain? A meta-analysis of
586 neuroimaging studies on spatial cognition. *Human Brain Mapping*, 40(6), 1867-1886.
587 <https://doi.org/10.1002/hbm.24496>
- 588 Coughlan, G., Laczó, J., Hort, J., Minihane, A.-M., & Hornberger, M. (2018). Spatial navigation
589 deficits—Overlooked cognitive marker for preclinical Alzheimer disease? *Nature Reviews.*
590 *Neurology*, 14(8), 496-506. <https://doi.org/10.1038/s41582-018-0031-x>
- 591 de Condappa, O., & Wiener, J. M. (2014). Human place and response learning : Navigation strategy
592 selection, pupil size and gaze behavior. *Psychological Research*, 80(1), 82-93.
593 <https://doi.org/10.1007/s00426-014-0642-9>
- 594 Delaux, A., de Saint Aubert, J.-B., Ramanoël, S., Bécu, M., Gehrke, L., Klug, M., Chavarriaga, R.,
595 Sahel, J.-A., Gramann, K., & Arleo, A. (2021). Mobile brain/body imaging of landmark-based
596 navigation with high-density EEG. *European Journal of Neuroscience*, 54(12), 8256-8282.
597 <https://doi.org/10.1111/ejn.15190>
- 598 Delorme, A., & Makeig, S. (2004). EEGLAB : An open source toolbox for analysis of single-trial
599 EEG dynamics including independent component analysis. *Journal of Neuroscience Methods*,
600 134(1), 9-21. <https://doi.org/10.1016/j.jneumeth.2003.10.009>
- 601 Di Russo, F., Martínez, A., & Hillyard, S. A. (2003). Source Analysis of Event-related Cortical
602 Activity during Visuo-spatial Attention. *Cerebral Cortex*, 13(5), 486-499.
603 <https://doi.org/10.1093/cercor/13.5.486>
- 604 Dilks, D. D., Julian, J. B., Paunov, A. M., & Kanwisher, N. (2013). The Occipital Place Area Is
605 Causally and Selectively Involved in Scene Perception. *Journal of Neuroscience*, 33(4),
606 1331-1336. <https://doi.org/10.1523/JNEUROSCI.4081-12.2013>
- 607 Dolcos, F., Rice, H. J., & Cabeza, R. (2002). Hemispheric asymmetry and aging : Right hemisphere
608 decline or asymmetry reduction. *Neuroscience & Biobehavioral Reviews*, 26(7), 819-825.
609 [https://doi.org/10.1016/S0149-7634\(02\)00068-4](https://doi.org/10.1016/S0149-7634(02)00068-4)
- 610 Durteste, M., Delaux, A., Ariztégui, A., Cottureau, B., Sheynikhovich, D., Ramanoel, S., & Arleo, A.
611 (2023). *Age-related disparities in oscillatory dynamics within scene-selective regions during*
612 *spatial navigation*. <https://doi.org/10.1101/2023.10.16.562507>
- 613 Ekstrom, A. D. (2015). Why vision is important to how we navigate. *Hippocampus*, 25(6), 731-735.
614 <https://doi.org/10.1002/hipo.22449>
- 615 Ekstrom, A. D., Huffman, D. J., & Starrett, M. (2017). Interacting networks of brain regions underlie
616 human spatial navigation : A review and novel synthesis of the literature. *Journal of*
617 *Neurophysiology*, 118(6), 3328-3344. <https://doi.org/10.1152/jn.00531.2017>

- 618 Epstein, R. A., Patai, E. Z., Julian, J. B., & Spiers, H. J. (2017). The cognitive map in humans : Spatial
619 navigation and beyond. *Nature neuroscience*, *20*(11), 1504-1513.
620 <https://doi.org/10.1038/nn.4656>
- 621 Epstein, R., & Kanwisher, N. (1998). A cortical representation of the local visual environment.
622 *Nature*, *392*(6676), Article 6676. <https://doi.org/10.1038/33402>
- 623 Faubert, J. (2002). Visual perception and aging. *Canadian Journal of Experimental Psychology =*
624 *Revue Canadienne De Psychologie Experimentale*, *56*(3), 164-176.
625 <https://doi.org/10.1037/h0087394>
- 626 Fellingner, R., Gruber, W., Zauner, A., Freunberger, R., & Klimesch, W. (2012). Evoked traveling
627 alpha waves predict visual-semantic categorization-speed. *NeuroImage*, *59*(4), 3379-3388.
628 <https://doi.org/10.1016/j.neuroimage.2011.11.010>
- 629 Finnigan, S., O'Connell, R. G., Cummins, T. D. R., Broughton, M., & Robertson, I. H. (2011). ERP
630 measures indicate both attention and working memory encoding decrements in aging.
631 *Psychophysiology*, *48*(5), 601-611. <https://doi.org/10.1111/j.1469-8986.2010.01128.x>
- 632 Fischer, L. F., Mojica Soto-Albors, R., Buck, F., & Harnett, M. T. (2020). Representation of visual
633 landmarks in retrosplenial cortex. *eLife*, *9*, e51458. <https://doi.org/10.7554/eLife.51458>
- 634 Foo, P., Warren, W. H., Duchon, A., & Tarr, M. J. (2005). Do Humans Integrate Routes Into a
635 Cognitive Map ? Map- Versus Landmark-Based Navigation of Novel Shortcuts. *Journal of*
636 *Experimental Psychology: Learning, Memory, and Cognition*, *31*(2), 195-215.
637 <https://doi.org/10.1037/0278-7393.31.2.195>
- 638 Freunberger, R., Klimesch, W., Doppelmayr, M., & Höller, Y. (2007). Visual P2 component is related
639 to theta phase-locking. *Neuroscience Letters*, *426*(3), 181-186.
640 <https://doi.org/10.1016/j.neulet.2007.08.062>
- 641 Friedman, A., Kohler, B., Gunalp, P., Boone, A. P., & Hegarty, M. (2020). A computerized spatial
642 orientation test. *Behavior Research Methods*, *52*(2), 799-812. [https://doi.org/10.3758/s13428-](https://doi.org/10.3758/s13428-019-01277-3)
643 [019-01277-3](https://doi.org/10.3758/s13428-019-01277-3)
- 644 Gazzaley, A., Clapp, W., Kelley, J., McEvoy, K., Knight, R. T., & D'Esposito, M. (2008). Age-related
645 top-down suppression deficit in the early stages of cortical visual memory processing.
646 *Proceedings of the National Academy of Sciences of the United States of America*, *105*(35),
647 13122-13126. <https://doi.org/10.1073/pnas.0806074105>
- 648 Glover, G. H. (2011). Overview of Functional Magnetic Resonance Imaging. *Neurosurgery clinics of*
649 *North America*, *22*(2), 133-139. <https://doi.org/10.1016/j.nec.2010.11.001>
- 650 Gramann, K., Hohlefeld, F. U., Gehrke, L., & Klug, M. (2021). Human cortical dynamics during full-
651 body heading changes. *Scientific Reports*, *11*(1), Article 1. [https://doi.org/10.1038/s41598-](https://doi.org/10.1038/s41598-021-97749-8)
652 [021-97749-8](https://doi.org/10.1038/s41598-021-97749-8)
- 653 Greene, M. R., & Oliva, A. (2009). Recognition of natural scenes from global properties : Seeing the
654 forest without representing the trees. *Cognitive Psychology*, *58*(2), 137-176.
655 <https://doi.org/10.1016/j.cogpsych.2008.06.001>
- 656 Griffiths, B. J., Mayhew, S. D., Mullinger, K. J., Jorge, J., Charest, I., Wimber, M., & Hanslmayr, S.
657 (2019). Alpha/beta power decreases track the fidelity of stimulus-specific information. *eLife*,
658 *8*, e49562. <https://doi.org/10.7554/eLife.49562>
- 659 Gruber, W. R., Klimesch, W., Sauseng, P., & Doppelmayr, M. (2005). Alpha Phase Synchronization
660 Predicts P1 and N1 Latency and Amplitude Size. *Cerebral Cortex*, *15*(4), 371-377.
661 <https://doi.org/10.1093/cercor/bhh139>
- 662 Hamid, S. N., Stankiewicz, B., & Hayhoe, M. (2010). Gaze patterns in navigation : Encoding
663 information in large-scale environments. *Journal of Vision*, *10*(12), 28-28.
664 <https://doi.org/10.1167/10.12.28>

- 665 Hanslmayr, S., Staudigl, T., & Fellner, M.-C. (2012). Oscillatory power decreases and long-term
666 memory : The information via desynchronization hypothesis. *Frontiers in Human*
667 *Neuroscience*, 6. <https://www.frontiersin.org/articles/10.3389/fnhum.2012.00074>
- 668 Harel, A., Groen, I. I. A., Kravitz, D. J., Deouell, L. Y., & Baker, C. I. (2016). The temporal dynamics
669 of scene processing : A multi-faceted EEG investigation. *eNeuro*.
670 <https://doi.org/10.1523/ENEURO.0139-16.2016>
- 671 Harel, A., Nador, J. D., Bonner, M. F., & Epstein, R. A. (2022). Early Electrophysiological Markers of
672 Navigational Affordances in Scenes. *Journal of Cognitive Neuroscience*, 34(3), 397-410.
673 https://doi.org/10.1162/jocn_a_01810
- 674 Harris, M. A., & Wolbers, T. (2012). Ageing effects on path integration and landmark navigation.
675 *Hippocampus*, 22(8), 1770-1780. <https://doi.org/10.1002/hipo.22011>
- 676 Hartmeyer, S., Grzeschik, R., Wolbers, T., & Wiener, J. M. (2017). The Effects of Attentional
677 Engagement on Route Learning Performance in a Virtual Environment : An Aging Study.
678 *Frontiers in Aging Neuroscience*, 9.
679 <https://www.frontiersin.org/articles/10.3389/fnagi.2017.00235>
- 680 Hayasaka, S., & Nichols, T. E. (2004). Combining voxel intensity and cluster extent with permutation
681 test framework. *NeuroImage*, 23(1), 54-63. <https://doi.org/10.1016/j.neuroimage.2004.04.035>
- 682 Herrmann, C. S., Rach, S., Vosskuhl, J., & Strüber, D. (2014). Time-frequency analysis of event-
683 related potentials : A brief tutorial. *Brain Topography*, 27(4), 438-450.
684 <https://doi.org/10.1007/s10548-013-0327-5>
- 685 Hillyard, S. A., Vogel, E. K., & Luck, S. J. (1998). Sensory gain control (amplification) as a
686 mechanism of selective attention : Electrophysiological and neuroimaging evidence.
687 *Philosophical Transactions of the Royal Society of London. Series B, Biological Sciences*,
688 353(1373), 1257-1270. <https://doi.org/10.1098/rstb.1998.0281>
- 689 Hopf, J.-M., Vogel, E., Woodman, G., Heinze, H.-J., & Luck, S. J. (2002). Localizing visual
690 discrimination processes in time and space. *Journal of Neurophysiology*, 88(4), 2088-2095.
691 <https://doi.org/10.1152/jn.2002.88.4.2088>
- 692 Jacobs, J. (2014). Hippocampal theta oscillations are slower in humans than in rodents : Implications
693 for models of spatial navigation and memory. *Philosophical Transactions of the Royal Society*
694 *of London. Series B, Biological Sciences*, 369(1635), 20130304.
695 <https://doi.org/10.1098/rstb.2013.0304>
- 696 Jacobs, J., Korolev, I. O., Caplan, J. B., Ekstrom, A. D., Litt, B., Baltuch, G., Fried, I., Schulze-
697 Bonhage, A., Madsen, J. R., & Kahana, M. J. (2010). Right-lateralized Brain Oscillations in
698 Human Spatial Navigation. *Journal of Cognitive Neuroscience*, 22(5), 824-836.
699 <https://doi.org/10.1162/jocn.2009.21240>
- 700 Janzen, G., & van Turenout, M. (2004). Selective neural representation of objects relevant for
701 navigation. *Nature Neuroscience*, 7(6), Article 6. <https://doi.org/10.1038/nn1257>
- 702 Julian, J. B., Keinath, A. T., Marchette, S. A., & Epstein, R. A. (2018). The Neurocognitive Basis of
703 Spatial Reorientation. *Current Biology*, 28(17), R1059-R1073.
704 <https://doi.org/10.1016/j.cub.2018.04.057>
- 705 Kaiser, D., Häberle, G., & Cichy, R. M. (2020). Cortical sensitivity to natural scene structure. *Human*
706 *Brain Mapping*, 41(5), 1286-1295. <https://doi.org/10.1002/hbm.24875>
- 707 Kalafat, M., Hugonot-Diener, L., & Poitrenaud, J. (2003). Standardisation et étalonnage français du
708 « Mini Mental State » (MMS) version GRÉCO. [French standardization and range for the
709 GRECO version of the « Mini Mental State » (MMS).]. *Revue de Neuropsychologie*, 13,
710 209-236.

- 711 Klencken, G., Després, O., & Dufour, A. (2012). What do we know about aging and spatial
712 cognition? Reviews and perspectives. *Ageing Research Reviews*, *11*(1), 123-135.
713 <https://doi.org/10.1016/j.arr.2011.10.001>
- 714 Klimesch, W. (1997). EEG-alpha rhythms and memory processes. *International Journal of*
715 *Psychophysiology: Official Journal of the International Organization of Psychophysiology*,
716 *26*(1-3), 319-340. [https://doi.org/10.1016/s0167-8760\(97\)00773-3](https://doi.org/10.1016/s0167-8760(97)00773-3)
- 717 Klimesch, W. (1999). EEG alpha and theta oscillations reflect cognitive and memory performance : A
718 review and analysis. *Brain Research Reviews*, *29*(2), 169-195. [https://doi.org/10.1016/S0165-0173\(98\)00056-3](https://doi.org/10.1016/S0165-0173(98)00056-3)
- 720 Klimesch, W. (2011). Evoked alpha and early access to the knowledge system : The P1 inhibition
721 timing hypothesis. *Brain Research*, *1408*, 52-71.
722 <https://doi.org/10.1016/j.brainres.2011.06.003>
- 723 Klimesch, W., Sauseng, P., & Hanslmayr, S. (2007). EEG alpha oscillations : The inhibition–timing
724 hypothesis. *Brain Research Reviews*, *53*(1), 63-88.
725 <https://doi.org/10.1016/j.brainresrev.2006.06.003>
- 726 Klimesch, W., Schack, B., Schabus, M., Doppelmayr, M., Gruber, W., & Sauseng, P. (2004). Phase-
727 locked alpha and theta oscillations generate the P1–N1 complex and are related to memory
728 performance. *Cognitive Brain Research*, *19*(3), 302-316.
729 <https://doi.org/10.1016/j.cogbrainres.2003.11.016>
- 730 Klug, M., & Gramann, K. (2021). Identifying key factors for improving ICA-based decomposition of
731 EEG data in mobile and stationary experiments. *European Journal of Neuroscience*, *54*(12),
732 8406-8420. <https://doi.org/10.1111/ejn.14992>
- 733 Klug, M., & Kloosterman, N. A. (2022). Zapline-plus : A Zapline extension for automatic and
734 adaptive removal of frequency-specific noise artifacts in M/EEG. *Human Brain Mapping*,
735 *43*(9), 2743-2758. <https://doi.org/10.1002/hbm.25832>
- 736 Koch, C., Li, S. C., Polk, T. A., & Schuck, N. W. (2020). Effects of aging on encoding of walking
737 direction in the human brain. *Neuropsychologia*.
738 <https://doi.org/10.1016/j.neuropsychologia.2020.107379>
- 739 Kothe, C. A. E., & Jung, T.-P. (2015). *Artifact removal techniques with signal reconstruction* (World
740 Intellectual Property Organization Brevet WO2015047462A9).
741 <https://patents.google.com/patent/WO2015047462A9/en>
- 742 Kravitz, D. J., Peng, C. S., & Baker, C. I. (2011). Real-World Scene Representations in High-Level
743 Visual Cortex : It's the Spaces More Than the Places. *Journal of Neuroscience*, *31*(20),
744 7322-7333. <https://doi.org/10.1523/JNEUROSCI.4588-10.2011>
- 745 Kropotov, J., Ponomarev, V., Tereshchenko, E. P., Müller, A., & Jäncke, L. (2016). Effect of Aging
746 on ERP Components of Cognitive Control. *Frontiers in Aging Neuroscience*, *8*, 69.
747 <https://doi.org/10.3389/fnagi.2016.00069>
- 748 Lai, L. Y., Frömer, R., Festa, E. K., & Heindel, W. C. (2020). Age-related changes in the neural
749 dynamics of bottom-up and top-down processing during visual object recognition : An
750 electrophysiological investigation. *Neurobiology of Aging*, *94*, 38-49.
751 <https://doi.org/10.1016/j.neurobiolaging.2020.05.010>
- 752 Learmonth, G., Benwell, C. S. Y., Thut, G., & Harvey, M. (2017). Age-related reduction of
753 hemispheric lateralisation for spatial attention : An EEG study. *NeuroImage*, *153*, 139-151.
754 <https://doi.org/10.1016/j.neuroimage.2017.03.050>
- 755 Lefebvre, C. D., Marchand, Y., Eskes, G. A., & Connolly, J. F. (2005). Assessment of working
756 memory abilities using an event-related brain potential (ERP)-compatible digit span backward
757 task. *Clinical Neurophysiology: Official Journal of the International Federation of Clinical*
758 *Neurophysiology*, *116*(7), 1665-1680. <https://doi.org/10.1016/j.clinph.2005.03.015>

- 759 Lester, A. W., Moffat, S. D., Wiener, J. M., Barnes, C. A., & Wolbers, T. (2017). The Aging
760 Navigational System. *Neuron*, 95(5), 1019-1035. <https://doi.org/10.1016/j.neuron.2017.06.037>
- 761 Li, J., Zhang, R., Liu, S., Liang, Q., Zheng, S., He, X., & Huang, R. (2021). Human spatial
762 navigation : Neural representations of spatial scales and reference frames obtained from an
763 ALE meta-analysis. *NeuroImage*, 238, 118264.
764 <https://doi.org/10.1016/j.neuroimage.2021.118264>
- 765 Lithfous, S., Dufour, A., Blanc, F., & Després, O. (2014). Allocentric but not egocentric orientation is
766 impaired during normal aging : An ERP study. *Neuropsychology*, 28(5), 761-771.
767 <https://doi.org/10.1037/neu0000084>
- 768 Lithfous, S., Dufour, A., Bouix, C., Pebayle, T., & Després, O. (2018). Reduced parahippocampal
769 theta activity during spatial navigation in low, but not in high elderly performers.
770 *Neuropsychology*, 32(1), 40-53. <https://doi.org/10.1037/neu0000392>
- 771 Luck, S. (2005). Ten simple rules for designing ERP Experiments. In *Event-Related Potentials : A*
772 *Methods Handbook* (p. 17-32).
- 773 Luck, S. J. (1995). Multiple mechanisms of visual-spatial attention : Recent evidence from human
774 electrophysiology. *Behavioural Brain Research*, 71(1-2), 113-123.
775 [https://doi.org/10.1016/0166-4328\(95\)00041-0](https://doi.org/10.1016/0166-4328(95)00041-0)
- 776 Luck, S. J. (2014). *An Introduction to the Event-Related Potential Technique, second edition*. MIT
777 Press.
- 778 Maguire, E. (2001). The retrosplenial contribution to human navigation : A review of lesion and
779 neuroimaging findings. *Scandinavian Journal of Psychology*, 42(3), 225-238.
780 <https://doi.org/10.1111/1467-9450.00233>
- 781 Makeig, S. (1993). Auditory event-related dynamics of the EEG spectrum and effects of exposure to
782 tones. *Electroencephalography and Clinical Neurophysiology*, 86(4), 283-293.
783 [https://doi.org/10.1016/0013-4694\(93\)90110-h](https://doi.org/10.1016/0013-4694(93)90110-h)
- 784 Marchette, S. A., Vass, L. K., Ryan, J., & Epstein, R. A. (2014). Anchoring the neural compass :
785 Coding of local spatial reference frames in human medial parietal lobe. *Nature Neuroscience*,
786 17(11), Article 11. <https://doi.org/10.1038/nn.3834>
- 787 Maris, E., & Oostenveld, R. (2007). Nonparametric statistical testing of EEG- and MEG-data. *Journal*
788 *of Neuroscience Methods*, 164(1), 177-190. <https://doi.org/10.1016/j.jneumeth.2007.03.024>
- 789 Mecklinger, A., Parra, M., & Waldhauser, G. T. (2009). ERP correlates of intentional forgetting. *Brain*
790 *Research*, 1255, 132-147. <https://doi.org/10.1016/j.brainres.2008.11.073>
- 791 Moca, V. V., Bârzan, H., Nagy-Dăbâcan, A., & Mureşan, R. C. (2021). Time-frequency super-
792 resolution with superlets. *Nature Communications*, 12(1), Article 1.
793 <https://doi.org/10.1038/s41467-020-20539-9>
- 794 Mueller, V., Brehmer, Y., von Oertzen, T., Li, S.-C., & Lindenberger, U. (2008). Electrophysiological
795 correlates of selective attention : A lifespan comparison. *BMC Neuroscience*, 9(1), 18.
796 <https://doi.org/10.1186/1471-2202-9-18>
- 797 Natale, E., Marzi, C. A., Girelli, M., Pavone, E. F., & Pollmann, S. (2006). ERP and fMRI correlates
798 of endogenous and exogenous focusing of visual-spatial attention. *The European Journal of*
799 *Neuroscience*, 23(9), 2511-2521. <https://doi.org/10.1111/j.1460-9568.2006.04756.x>
- 800 Oostenveld, R., Fries, P., Maris, E., & Schoffelen, J.-M. (2011). FieldTrip : Open source software for
801 advanced analysis of MEG, EEG, and invasive electrophysiological data. *Computational*
802 *Intelligence and Neuroscience*, 2011, 156869. <https://doi.org/10.1155/2011/156869>
- 803 Oostenveld, R., & Oostendorp, T. F. (2002). Validating the boundary element method for forward and
804 inverse EEG computations in the presence of a hole in the skull. *Human Brain Mapping*,
805 17(3), 179-192. <https://doi.org/10.1002/hbm.10061>

- 806 Palmer, J. A., Makeig, S., Kreutz-Delgado, K., & Rao, B. D. (2008). Newton method for the ICA
807 mixture model. *2008 IEEE International Conference on Acoustics, Speech and Signal*
808 *Processing*, 1805-1808. <https://doi.org/10.1109/ICASSP.2008.4517982>
- 809 Persichetti, A. S., & Dilks, D. D. (2018). Dissociable Neural Systems for Recognizing Places and
810 Navigating through Them. *Journal of Neuroscience*, *38*(48), 10295-10304.
811 <https://doi.org/10.1523/JNEUROSCI.1200-18.2018>
- 812 Persichetti, A. S., & Dilks, D. D. (2019). Distinct representations of spatial and categorical
813 relationships across human scene-selective cortex. *Proceedings of the National Academy of*
814 *Sciences*, *116*(42), 21312-21317. <https://doi.org/10.1073/pnas.1903057116>
- 815 Philips, S., & Takeda, Y. (2009). An EEG/ERP study of efficient versus inefficient visual search.
816 *Proceedings of the Annual Meeting of the Cognitive Science Society*, *31*(31).
817 <https://escholarship.org/uc/item/93x9f8bb>
- 818 Pion-Tonachini, L., Kreutz-Delgado, K., & Makeig, S. (2019). ICLabel : An automated
819 electroencephalographic independent component classifier, dataset, and website. *NeuroImage*,
820 *198*, 181-197. <https://doi.org/10.1016/j.neuroimage.2019.05.026>
- 821 Plewan, T., & Rinkenauer, G. (2017). Simple reaction time and size–distance integration in virtual 3D
822 space. *Psychological Research*, *81*(3), 653-663. <https://doi.org/10.1007/s00426-016-0769-y>
- 823 Ramanoël, S., Durteste, M., Bécu, M., Habas, C., & Arleo, A. (2020). Differential Brain Activity in
824 Regions Linked to Visuospatial Processing During Landmark-Based Navigation in Young and
825 Healthy Older Adults. *Frontiers in Human Neuroscience*, *14*.
826 <https://www.frontiersin.org/articles/10.3389/fnhum.2020.552111>
- 827 Ramanoël, S., Durteste, M., Bizeul, A., Ozier-Lafontaine, A., Bécu, M., Sahel, J.-A., Habas, C., &
828 Arleo, A. (2022). Selective neural coding of object, feature, and geometry spatial cues in
829 humans. *Human Brain Mapping*, *43*(17), 5281-5295. <https://doi.org/10.1002/hbm.26002>
- 830 Ramanoël, S., Kauffmann, L., Cousin, E., Dojat, M., & Peyrin, C. (2015). Age-related differences in
831 spatial frequency processing during scene categorization. *PLoS ONE*.
832 <https://doi.org/10.1371/journal.pone.0134554>
- 833 Ramanoël, S., York, E., Le Petit, M., Lagrené, K., Habas, C., & Arleo, A. (2019). Age-Related
834 Differences in Functional and Structural Connectivity in the Spatial Navigation Brain
835 Network. *Frontiers in Neural Circuits*, *13*.
836 <https://www.frontiersin.org/articles/10.3389/fncir.2019.00069>
- 837 Ryan, J. D., Wynn, J. S., Shen, K., & Liu, Z.-X. (2022). Aging changes the interactions between the
838 oculomotor and memory systems. *Neuropsychology, Development, and Cognition. Section B,*
839 *Aging, Neuropsychology and Cognition*, *29*(3), 418-442.
840 <https://doi.org/10.1080/13825585.2021.2007841>
- 841 Sawetsuttipan, P., Phunchongharn, P., Ounjai, K., Salazar, A., Pongsuwan, S., Intrachotoo, S.,
842 Serences, J. T., & Itthipuripat, S. (2023). Perceptual Difficulty Regulates Attentional Gain
843 Modulations in Human Visual Cortex. *The Journal of Neuroscience: The Official Journal of*
844 *the Society for Neuroscience*, *43*(18), 3312-3330. [https://doi.org/10.1523/JNEUROSCI.0519-](https://doi.org/10.1523/JNEUROSCI.0519-22.2023)
845 [22.2023](https://doi.org/10.1523/JNEUROSCI.0519-22.2023)
- 846 Segen, V., Avraamides, M. N., Slattery, T. J., & Wiener, J. M. (2021). Age-related differences in
847 visual encoding and response strategies contribute to spatial memory deficits. *Memory &*
848 *Cognition*, *49*(2), 249-264. <https://doi.org/10.3758/s13421-020-01089-3>
- 849 Silson, E. H., Steel, A. D., & Baker, C. I. (2016). Scene-Selectivity and Retinotopy in Medial Parietal
850 Cortex. *Frontiers in Human Neuroscience*, *10*, 412.
851 <https://doi.org/10.3389/fnhum.2016.00412>
- 852 Sperandio, I., Savazzi, S., Gregory, R. L., & Marzi, C. A. (2009). Visual Reaction Time and Size
853 Constancy. *Perception*, *38*(11), 1601-1609. <https://doi.org/10.1068/p6421>

- 854 Spitzer, B., & Haegens, S. (2017). Beyond the Status Quo : A Role for Beta Oscillations in
855 Endogenous Content (Re)Activation. *eNeuro*, 4(4). [https://doi.org/10.1523/ENEURO.0170-](https://doi.org/10.1523/ENEURO.0170-17.2017)
856 [17.2017](https://doi.org/10.1523/ENEURO.0170-17.2017)
- 857 Srokova, S., Hill, P. F., Koen, J. D., King, D. R., & Rugg, M. D. (2020). Neural differentiation is
858 moderated by age in scene-selective, but not face-selective, cortical regions. *eNeuro*, 7(3).
859 <https://doi.org/10.1523/ENEURO.0142-20.2020>
- 860 Sun, L., Frank, S. M., Epstein, R. A., & Tse, P. U. (2021). The parahippocampal place area and
861 hippocampus encode the spatial significance of landmark objects. *NeuroImage*, 236, 118081.
862 <https://doi.org/10.1016/j.neuroimage.2021.118081>
- 863 Van der Lubbe, R. H. J., Szumska, I., & Fajkowska, M. (2016). Two Sides of the Same Coin : ERP
864 and Wavelet Analyses of Visual Potentials Evoked and Induced by Task-Relevant Faces.
865 *Advances in Cognitive Psychology*, 12(4), 154-168. <https://doi.org/10.5709/acp-0195-3>
- 866 Vann, S. D., Aggleton, J. P., & Maguire, E. A. (2009). What does the retrosplenial cortex do? *Nature*
867 *Reviews Neuroscience*, 10(11), Article 11. <https://doi.org/10.1038/nrn2733>
- 868 Vlcek, K., Fajnerova, I., Nekovarova, T., Hejtmanek, L., Janca, R., Jezdik, P., Kalina, A., Tomasek,
869 M., Krsek, P., Hammer, J., & Marusic, P. (2020). Mapping the Scene and Object Processing
870 Networks by Intracranial EEG. *Frontiers in Human Neuroscience*, 14, 561399.
871 <https://doi.org/10.3389/fnhum.2020.561399>
- 872 Vogel, E. K., & Luck, S. J. (2000). The visual N1 component as an index of a discrimination process.
873 *Psychophysiology*, 37(2), 190-203.
- 874 Warbrick, T., Arrubla, J., Boers, F., Neuner, I., & Shah, N. J. (2014). Attention to Detail : Why
875 Considering Task Demands Is Essential for Single-Trial Analysis of BOLD Correlates of the
876 Visual P1 and N1. *Journal of Cognitive Neuroscience*, 26(3), 529-542.
877 https://doi.org/10.1162/jocn_a_00490
- 878 Wenzel, F., Hepperle, L., & von Stülpnagel, R. (2017). Gaze behavior during incidental and
879 intentional navigation in an outdoor environment. *Spatial Cognition and Computation*,
880 17(1-2). <https://doi.org/10.1080/13875868.2016.1226838>
- 881 West, G. L., Patai, Z. E., Coutrot, A., Hornberger, M., Bohbot, V. D., & Spiers, H. J. (2023).
882 Landmark-dependent Navigation Strategy Declines across the Human Life-Span : Evidence
883 from Over 37,000 Participants. *Journal of Cognitive Neuroscience*, 35(3), 452-467.
884 https://doi.org/10.1162/jocn_a_01956
- 885 Wiegand, I., Töllner, T., Dyrholm, M., Müller, H. J., Bundesen, C., & Finke, K. (2014). Neural
886 correlates of age-related decline and compensation in visual attention capacity. *Neurobiology*
887 *of Aging*, 35(9), 2161-2173. <https://doi.org/10.1016/j.neurobiolaging.2014.02.023>
- 888 Wiener, J., Kmecova, H., & de Condappa, O. (2012). Route repetition and route retracing : Effects of
889 cognitive aging. *Frontiers in Aging Neuroscience*, 4.
890 <https://www.frontiersin.org/articles/10.3389/fnagi.2012.00007>
- 891 Wolbers, T., & Hegarty, M. (2010). What determines our navigational abilities? *Trends in Cognitive*
892 *Sciences*, 14(3), 138-146. <https://doi.org/10.1016/j.tics.2010.01.001>
- 893 Young, A. (2012). *Functions of the Right Cerebral Hemisphere*. Elsevier.
- 894 Zhang, H., Copara, M., & Ekstrom, A. D. (2012). Differential Recruitment of Brain Networks
895 following Route and Cartographic Map Learning of Spatial Environments. *PLOS ONE*, 7(9),
896 e44886. <https://doi.org/10.1371/journal.pone.0044886>
- 897